Title
Quantifying biogeochemical heterogeneity in soil systems

Authors
Wanzek, Thomas
Keiluweit, Marco
Baham, John
et al.

Publication Date
2018-08-01

DOI
10.1016/j.geoderma.2018.03.003

Peer reviewed

Quantifying biogeochemical heterogeneity in soil systems

Thomas Wanzek[a] Marco Keiluweit[b] John Baham[a] Maria I. Dragila[a] Scott Fendorf[c] Sabine Fiedler[d] Peter S. Nico[e] Markus Kleber[a]

Abstract

Soils are increasingly perceived as complex systems with properties and biogeochemical functions that vary on millimeter scales. Quantitative information about the resulting biogeochemical heterogeneity is needed to improve process knowledge and to render biogeochemical models more mechanistic. Here we demonstrate how standardized arrays of Pt-electrodes can be used to quantify biogeochemical or ‘functional’ soil heterogeneity, defined as the extent to which the soil is subdivided into microenvironments. Our case study confirmed the validity of this approach for a soil sequence consisting of a well-drained, a moderately well drained and a poorly drained Mollisol. We found that (i) variations in soil moisture content are the immediate cause for variations in functional heterogeneity, with (ii) soil porosity influencing rates and the magnitude of change. We posit that the deployment of standardized arrays of Pt-electrodes will offer an affordable option to monitor the general metabolic state of the soil system and simultaneously quantify the functional heterogeneity of underlying processes at any point in time. Such information should be useful to improve quantitative estimates of processes as diverse as trace gas emissions, trace gas consumption, reductive dehalogenation and mobilization of metals in the subsurface biosphere.

We recommend that parameterization of functional soil heterogeneity be included in long-term soil monitoring programs such as Superfund Sites, Critical Zone Observatories, Long Term Ecological Research (LTER) and National Ecological Observatory Network (NEON) sites.

Keywords: Biogeochemical heterogeneity, Soil microenvironments, Redox conditions, Platinum electrode, Electromotive potential, Metabolic heterogeneity index

1. Introduction

1.1. Soils are assemblies of functionally dissimilar microenvironments

Soil is a porous medium necessary to support plant and animal life in the terrestrial biosphere. Soil borne fauna and flora of all sizes and lifestyles continuously rework the mineral-organic soil
matrix, rendering its pore network highly random and inherently transitory. Because habitat form (pore size and morphology) affects (microbial) function, the resulting functional heterogeneity within "the most complicated biomaterial on the planet" (Young and Crawford, 2004) poses a problem when it becomes necessary to assess the direction and intensity of the processes that cycle biologically important elements such as C, N, P and S at a given site. Variations in soil structure induce variations in system behavior,

with the consequence that a given biogeochemical reaction may be logistically and energetically possible in one pore while inhibited in the pore right next to it. For instance, Kravchenko et al. (2015) show that losses of particulate organic matter were 3–15 times higher from atmosphere-connected soil pores than in isolated pores, while Negassa et al. (2015) demonstrated a dependence of microbial community composition on physical pore characteristics. Recognition of functional heterogeneity has given rise to the concept of biogeochemical hot spots and hot moments (Kuzyakov and Blagodatskaya, 2015; McClain et al., 2003) and has prompted calls to develop means for the robust quantification of soil heterogeneity across scales (Groffman et al., 2009; Vereecken et al., 2016).

Microenvironments can be functionally distinguished from the surrounding environment by the intensity (McClain et al., 2003) and type (Keiluweit et al., 2016; Sexstone et al., 1985) of the microbially mediated geochemical reactions they harbor. Here it is useful to remember that the vast majority of the chemical reactions occurring in environmental systems are oxidation - reduction reactions, i.e., processes that involve the transfer of electrons from an electron donor (such as reduced organic matter) to an electron acceptor (such as ferric iron, Fe^{3+}). Electrons can thus be considered as essential reactants in oxidation-reduction reactions (Bohn, 1971). Here we propose to quantify functional heterogeneity in soil environments by leveraging information on the electrochemical potential of a given microenvironment.

Our overarching **goal** is to develop a quantitative means to describe the extent to which a given soil volume may be subdivided into biogeochemically distinct microsites. We assumed that functional heterogeneity would express itself as a variation in the electron activity within a given soil volume that can be captured with a geometrically fixed array of multiple electrodes. We then develop a numerical indicator value for the extent to which a given soil volume is subdivided into biogeochemically distinct microsites.
Our **objectives** were to demonstrate the validity of our assumptions for a set of hydrologically different soils and to explore the importance of external controls (precipitation, temperature and height of the water table) for the formation of functionally distinct microenvironments. To this end, we examined functional heterogeneity along a gradient extending from well drained over moderately well drained to poorly drained soils.

Specifically, we **hypothesized** that

(i)

functional heterogeneity increases along a drainage gradient with increasingly wetter soil moisture regime,

(ii)

functional heterogeneity decreases with soil depth and

(iii)

functional heterogeneity in soil systems is a function of external environmental drivers and hence not constant over time.

1.2. Measuring electron activities: the Pt-electrode approach

Contemporary methods to characterize soil three-dimensional structure are increasingly allowing us to observe variations in microbial metabolism at the submicron scale, but there is a lack of robust, quantitative information about the spatial and temporal distribution of physiologically diverse microenvironments at the mm to cm (meso-)scale. A microscaleobservation requiring that a sample be taken to an elaborate research facility such as a synchrotron and there examined for several hours cannot easily be replicated at the frequency necessary to make valid inference about a watershed or a landscape. While we can observe processes at the submicron scale as well as at the much larger watershed or landscape scale, we still lack the ability to express the latter as a function of the former, mainly because we do not yet have a practical means to enter the parameter "soil heterogeneity" into testable scaling laws that would allow us to bridge the scale gap.

Our suggestion to use Pt-electrode potentials for the identification of functionally different soil microsites stems from early observations that replicate Pt-electrodes deployed in the same soil horizon do not typically return the same electromotive potential but may deviate by >300 mV (McKeague, 1965). While sometimes attributed to technical deficiencies of the Pt-electrode as discussed below, the phenomenon was further examined by Cogger et al. (1992) and Fiedler (1999) (Fig. 7.1 therein). Fiedler installed replicate Pt-electrodes at a distance of 10 mm in the topsoil (5 cm depth) of a Humaquept and found the potentials returned to be close during summer but to deviate up to 800 mV during periods of high rainfall and snowmelt. Corroborating the assessment of Cogger et al. (1992), Fiedler (1999)concluded that soil microsites are the primary source of variability among properly constructed and maintained electrodes. The operational consequence of these findings was the practice of subsequent workers to install multiple electrodes per same depth, thereby obtaining a more robust indicator for the general redox state of the soil horizon or soil depth of interest (Austin and Huddleston, 1999; Dorau and Mansfeldt, 2016; Dwire et al., 2006; Faulkner and Patrick, 1992; Faulkner et al., 1989; Fiedler and Kalbitz, 2003; Mansfeldt, 2003; Mansfeldt, 2004; Megonigal et al., 1993; Seybold et al., 2002; Vepraskas and Faulkner, 2001; Yu et al., 2006).

Table 1. Symbols, definitions and associated equations.

Symbol	Definition	Equation/unit
x_{ij}	Single data point; value returned by electrode i on day j	mV
a	Number of electrodes per individual linear array.	a = 5 = constant, distance

Symbol	Definition	Equation/unit
		between electrodes = 10 cm
J	Number of observation time points	J = # of days and observations per observation period
1.) Variability within one array, single observation point j		
$\mu_{(aj)}$ (Fig. 5)	Mean electromotive potential among 5 electrodes within one array on day j	$\mu aj = \sum xija$
$s_{(aj)}$ (Fig. 5)	standard deviation of the mean within one electrode array on day j	$Saj = 1a \sum i=1a xij - \mu aj2$
2.) Variability within one array and depth		
$\mu_{(D)}$ (Fig. 6)	Mean electromotive potential at depth D for J = 37 days	$\mu D = \sum xijJ$
$s_{(D)}$ (Fig. 6)	Standard deviation of the mean at depth D for J = 37 days	$sD = 1J \sum i=1J xij - \mu D2$
3.) Dimension of and changes in variability		
$\mu[s_{(aj)}]$ (Fig. 7)	Mean variability at a given depth D for J = 18 days	$\mu saj = \sum sajJ$
$s[s_{(aj)}]$ (Fig. 7)	Standard deviation of the variability at depth D for J = 18 days	$ssaj = 1J \sum i=1J saj - \mu saj2$

With the work presented here, we take the insight that Pt-electrodes are able to sense the existence of functionally different soil microsites as an opportunity to quantitatively assess the biogeochemical or ‘functional’ heterogeneity of soil. We argue that, if related to an array of geometrically related observation points, the heterogeneity of metabolic conditions within the soil volume defined by such an array can be conveniently expressed using descriptive statistics, effectively providing us with a metric for functional diversity within that soil volume.

It must be emphasized that the electromotive potentials thus obtained are not accurate predictors for the speciation of given redox couples in the soil system (Chapelle et al., 1996; Mansfeldt, 2004; Stumm, 1966). This limitation arises from both, (i) systemic issues related to the chemical

complexity of the soil system and (ii) restrictions resulting from the properties of the electrodes used to measure the potential. Briefly, measurements of electromotive potentials in soils are complicated by the simultaneous presence of multiple redox couples in the soil system giving rise to 'mixed potentials', by a dependence on soil pH, by slow kinetics of important potential-determining redox couples at the electrode and by the lack of chemical equilibrium among various redox couples (Sigg, 1999; Stumm, 1966). These systemic constraints are further complicated by the propensity of the Pt-electrode to chemically react with oxygen, to exhibit voltage drift and to experience fouling under conditions as reviewed by James and Brose (2011). As a result, a comparison of published data for natural environments (Fig. 1) suggests measurements of electromotive potentials in soil can certainly indicate a general disposition of a soil system towards given redox reactions but no clear delineations between different soil redox states. For instance (Fig. 1), the first appearance of Mn^{2+} in a cohort of 9 independent investigations carried out in different soils and settings occurred at an apparent Pt-electrode potential of +700 mV in one study but ranged all the way down to +200 mV in another report.

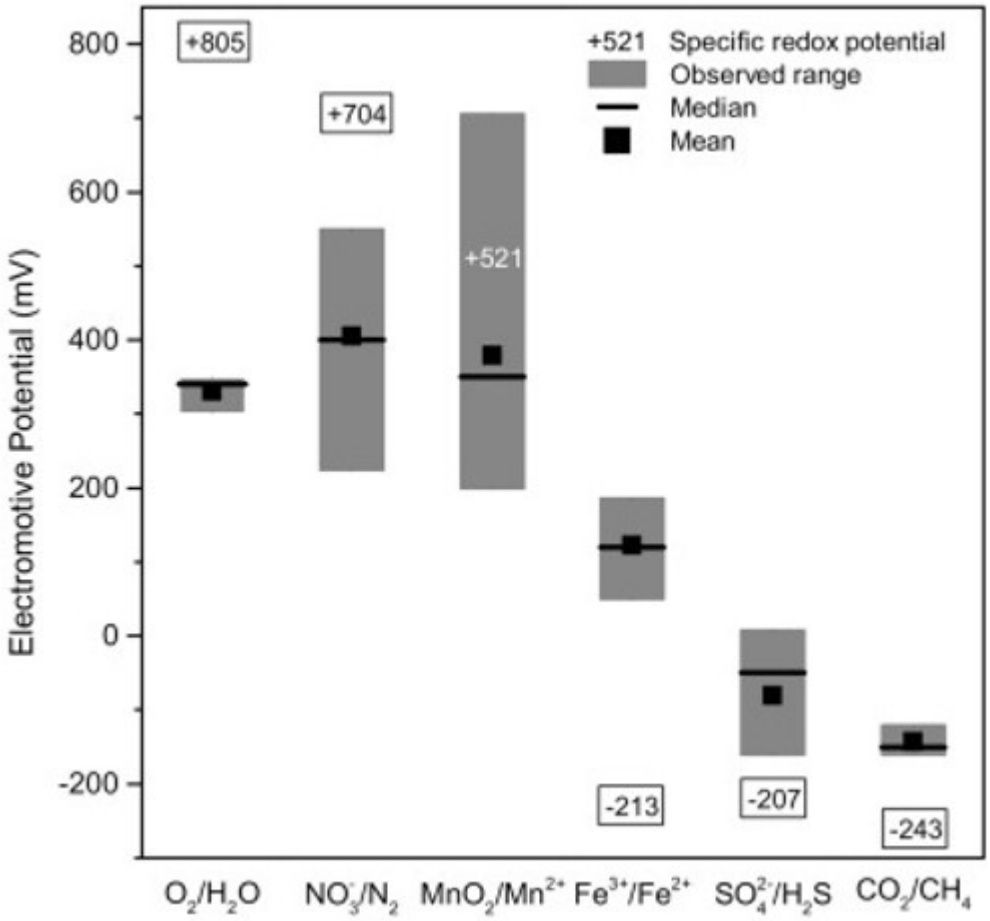

Fig. 1. Disparity between specific redox potentials for common redox couples and the experimentally observed range for the first appearance of the reduced species in soils as a function of increasing electron activity following inundation. $N = 9$ independent studies all using platinum electrodes (Brümmer, 1974; Gotoh and Yamashita, 1966; Kofod, 1999; Mansfeldt, 2004; Patrick and Jugsujinda, 1992; Patrick and Mahapatra, 1968; Patrick and Turner, 1968; Wang et al., 1993; Yu et al., 2007). For the oxygen/water couple, the range of values below which O_2 was no longer detectable is given and $n = 3$). Oxygen data from Patrick and Turner (1968), Patrick and Jugsujinda (1992), and Yu et al. (2006). All studies were either conducted at pH values close to 7 or the data were published including a correction to pH 7. Specific redox potentials from James and Brose (2011) representing conditions of $pH = 7$, $[red] = [ox] = 10^{-4}$ M, 0.21 atm for O_2, 0.78 atm for N_2, and 0.00032 atm for CO_2.

Clearly, this prevents the user from making robust predictions about the speciation of Mn in soils returning potentials above +200 mV. The scientific community has long been engaged in a debate as to the value of such information. While some question the usefulness of Pt-electrodes for electromotive potential measurements in soil altogether (Bartlett and James, 1995; Peiffer, 1992; Peiffer, 1999; Sposito, 2016), others point at obvious correlations of Pt-electrode derived electromotive potentials with soil morphology (Chadwick and Chorover, 2001; Fiedler and Sommer, 2004; Patrick et al., 1996), element distributions (Fiedler and Sommer, 2004; Mansfeldt, 2004; Masscheleyn et al., 1990) pedogenic thresholds of Fe, P and S (Chacon et al., 2006; Dorau and Mansfeldt, 2016; Gomez et al., 1999), methaneproduction (Fiedler and Sommer, 2000; Wang et al., 1993; Yu et al., 2007) and even suggest the use of Pt-electrode potentials as agricultural planning tools (Husson, 2012; Husson et al., 2016). For the purpose of this study, we refrain from any specific inference regarding the abundance of certain chemical species or from inference for microbial ecology in the sense of Baas Becking et al. (1960), but use electromotive potentials solely as unspecific proxies to establish the existence and the magnitude of functional differences between soil microenvironments.

To parameterize functional heterogeneity, we installed linear arrays of five equidistant (10 cm) Pt-electrodes at four depths (10, 20, 50 and 100 cm) in each soil. The magnitude of the standard deviation of the mean ($n = 5$) electromotive potential among the electrodes at a given observation instance then represents the biogeochemical heterogeneity of the soil along a horizontal distance of 40 cm. The electrode tips (Fig. A.4) were hypothesized to probe a microenvironment of the size of a few mm^3 (Fiedler et al., 2007). To capture seasonal variations, electromotive potentials were recorded several times a week for a period of 18 months, including two wet winter seasons.

2. Methods

2.1. Site and soil properties

Our **conceptual approach** consisted of selecting three soils in a way that they were derived from the same parent material, belonged to the same taxonomic soil order (Mollisols), were spatially close enough to be considered

as being under the exact same climate regime but represented a gradient in soil moisture regime between soils.

The drainage classes used by NRCS-USDA (Schoeneberger et al., 2012) refer to the frequency and duration of wet periods under conditions similar to those under which the soil developed. A soil is classified as **well drained** when water is removed readily and the soil is free of redoximorphic features. In a **moderately well drained soil**, water is removed somewhat slowly during some periods of the year, allowing for weak hydromorphic features to develop. Hydraulic conductivity is lower than in a well-drained soil. As a result of very low saturated hydraulic conductivity, **poorly drained soils** are wet at shallow depths periodically or for extended periods, allowing for the development of prominent hydromorphic features.

The three research sites were located in the central part of the Willamette Valley, 7 miles north east of the Oregon State University campus in Corvallis, Oregon (Fig. A.1). The Willamette Valley is a broad level plain in western Oregon that lies to the east of the Coast Range Mountains. Complex soil stratigraphy related to interfingering of Late Pleistocene glacial flood deposits (Balster and Parsons, 1968) combined with postglacial pedogenic clay translocation results in physical discontinuities within the solum that strongly influence transmission or lack of transmission of water (Austin and Huddleston, 1999; Boersma et al., 1972). The rain shadow of the Coast Range allows for an average of 900 mm of precipitation between October and May (Fall/Winter/Spring), and only 80 mm during June, July, August, and September. Mean air temperature averages 4 °C in January and 19 °C in July.

Two of the sites (Willamette and Amity) were on a USDA managed research farm and the third immediately adjacent on Hyslop Research Farm (Woodburn), which is part of the Oregon State University College of Agricultural Sciences – Corvallis Farm Unit. The Willamette soil is a well-drained Pachic Ultic Argixeroll, the Woodburn is a moderately well drained Aquultic Argixeroll and the Amity is classified as a poorly drained Argiaquic Xeric Argialboll (Soil Survey Staff, 2015). The three sites were about one and a half miles apart, were situated on spots adjacent to but outside of active research fields, had been unmanaged for >10 years with the exception of biannual mowing and all had a largely constant grassland vegetation mix dominated by *Agrostis capillaris*, Agrostis stolonifera and *Hypochaeris radicata*. Soil reaction across the profiles was similar with a gradient from pH 5.5 ± 0.07 in the topsoil to pH 6.3 ± 0.28 at 100 cm depth (mean ± SD from all three soils). All three series share a similar overall texture class (silt-loam), but bulk density was variable with a trend towards denser horizons from Willamette over Woodburn towards Amity. Basic soil properties are given in Table A.2.

2.2. Measurement of electromotive potentials

Two types of Pt-electrodes were used in this study. Woodburn and Amity were instrumented first, with electrodes similar to those described by Fiedler

et al. (2007). The need to obtain 20 additional probes for the monitoring of the Willamette soil was taken as an opportunity to miniaturize the Pt-electrodes for the purpose of lesser soil disturbance while maintaining the same functionality and durability as the larger electrodes. Briefly, 1.5 cm lengths of 16 ga. 99.95% pure platinum wire (Surepure Chemetals, Florham Park, NJ USA) were soldered, using light duty rosin core solder (Radio Shack, Fort Worth, TX USA), to two meter lengths of insulated 16 ga. copper wire. The Pt – Cu junction was then encased in low conductivity, clear epoxy casting resin (Alumilite Corp., Kalamazoo, MI USA) for increased stability and protection. Prior to installation in the field, each Pt-electrode was tested against a quinhydrone solution (0.1 g quinhydrone per 50 ml deionized water) buffered to pH 7. If the measured potential was more than +/− 10 mV outside of the ideal potential at 20 °C (92 mV), the probe was cleaned and retested (Austin and Huddleston, 1999; Jones, 1966) After successful testing, Pt-electrodes were installed at depths of 10, 20, 50 and 100 cm in linear arrays of 5 Pt-electrodes each. Electrode arrays had a horizontal extension of 40 cm and a distance between individual Pt-electrodes of 10 cm. The tip of each Pt-electrode was inserted horizontally into the pit wall to a distance of 10 cm from the wall face. Once installed in the field, the electrode leads were gathered and protected in a closable junction box. All electrodes were given two weeks to equilibrate in situ prior to the start of data collection. E_{Pt}data was collected manually every other day beginning in January 2015 through April 2016.

Potentials were collected manually using a Fluke 27 digital multi-meter (DMM, Fluke Corporation, Everett, WA USA), a custom-built resistance amplifier (detailed below), and a 3 M Ag/AgCl InLab reference electrode (Mettler and Toledo, Columbus, OH USA). Field measurements were normalized relative to the standard hydrogen electrode by adding a correction factor calculated for each measurement and depth using daily soil temperaturedata (Nordstrom and Wilde, 2005). E_{Pt} data are reported based on actual soil pH as reported in Table A.2. Inexpensive DMMs have low input resistance ($\sim 10^6\,\Omega$), which makes measurements of electromotive potentials in low voltage systems such as soils unreliable (Fiedler et al., 2007; Rabenhorst, 2009) as an unpredictable drop in voltage can occur when current flows from the soil microenvironment through the DMM. To remedy this issue, Wanzek built a one-off resistance amplifier to increase the input resistance of the hand held DMM from $10^6\,\Omega$ to $>10^{13}\,\Omega$ (Fig. A.2) following the design proposed by Rabenhorst (2009). The resistance amplifier was designed to be self-contained and utilized a TLE2426 precision virtual ground operational amplifier from Texas Instruments (Dallas, TX USA), one 9 V battery, and an on/off switch (to preserve battery life). Functionality of the resistance amplifier was tested and asserted in a 6-week test campaign by plotting corrected (plus amplifier) versus raw (minus amplifier) data to find the same magnitude of deviations as in Rabenhorst (2009; data not shown).

2.3. Soil moisture content and soil temperature

Volumetric water content and soil temperature was monitored at each depth in the Woodburn and Amity soils using Decagon 5TE soil moisture sensors ($n = 1$, with the exception of Woodburn 10, Woodburn 20, Amity 20 and Amity 50, where $n = 2$). Data were recorded every six hours on Decagon EM50 data-loggers (Decagon Devices, Pullman, WA USA). Water filled pore space was then calculated for each depth in the Woodburn and Amity soils using volumetric water content (VWC) and percent porosity, which was calculated using bulk density data.

Pt-electrodes and Decagon sensors were installed in the Woodburn and Amity soils in January 2015. A total absence of any redoximorphic features in the Willamette soil prompted us to initially focus our resources on the wetter soils of our sequence. Hence instrumentation of the Willamette soil with Pt-electrodes was delayed until the beginning of the 2015/16 wet season and no Decagon sensors were installed.

2.4. Climate data

Climate data were recorded daily by a weather station installed at Hyslop Farm and managed by the National Oceanic and Atmospheric Administration (NOAA) as a part of their Global Historical Climatology Network (Menne et al., 2012). Data were downloaded through the National Climatic Data Center's Climate Data Online tool. The depth to standing water in the Amity soil pit was measured from ground level at each E_{Pt} data collection event. There was no standing water at the level of the electrodes in the Woodburn and Willamette at any point in time.

2.5. Soil pH

Soil samples for pH measurement were collected once per month from each soil and depth from January 2015 through May 2015. Using a 5 cm by 10 cm bucket auger, about 200 cm^3 of soil was removed at each sampling event ($n = 5$ sampling events for the Woodburn and Amity and $n = 4$ for the Willamette). Samples were manually homogenized and large root matter was removed. A slurry was prepared at a 2:1 water/soil ratio and pH was measured using an Accumet AB15 pH meter and gel probe (Fisher Scientific, Waltham, MA USA). Monthly pH measurements were discontinued when no significant change over time was observed.

3. Results

3.1. Environmental drivers and electron activities

3.1.1. Precipitation

Cumulative rainfall data comparing the wet season of 2015 with the wet season of 2016 is given in Table A.3, showing that winter 2015 was much drier (378 mm for the period from January–April) than winter 2016 (601 mm for the same period). With a total pore space in the order of $500\ L\ m^{-2}\ m^{-1}$ (Table A.2), the precipitation values indicate a potential for whole profile saturation in the year 2016 but not for the winter of 2015. The

highest monthly precipitation total was observed in December 2015 (354.9 mm) and the lowest in July 2015 (0 mm). While there were fewer precipitation events in winter 2015 than in 2016, the proportion of intense rainfall events (>30 l m^{-2}) was greater. Overall, on six occasions (Fig. 2, panel a), daily rainfall reached or exceeded 30 l m^{-2}. Two of these events occurred in the first wet season: one in mid-January 2015 (41.1 mm) and one in mid-March 2015 (44.5 mm). The remaining four events preceded the second wet season: one occurred in late October 2015 (30.5 mm) and three in December 2015 (30.2 mm, 42.4 mm, and 49.8 mm).

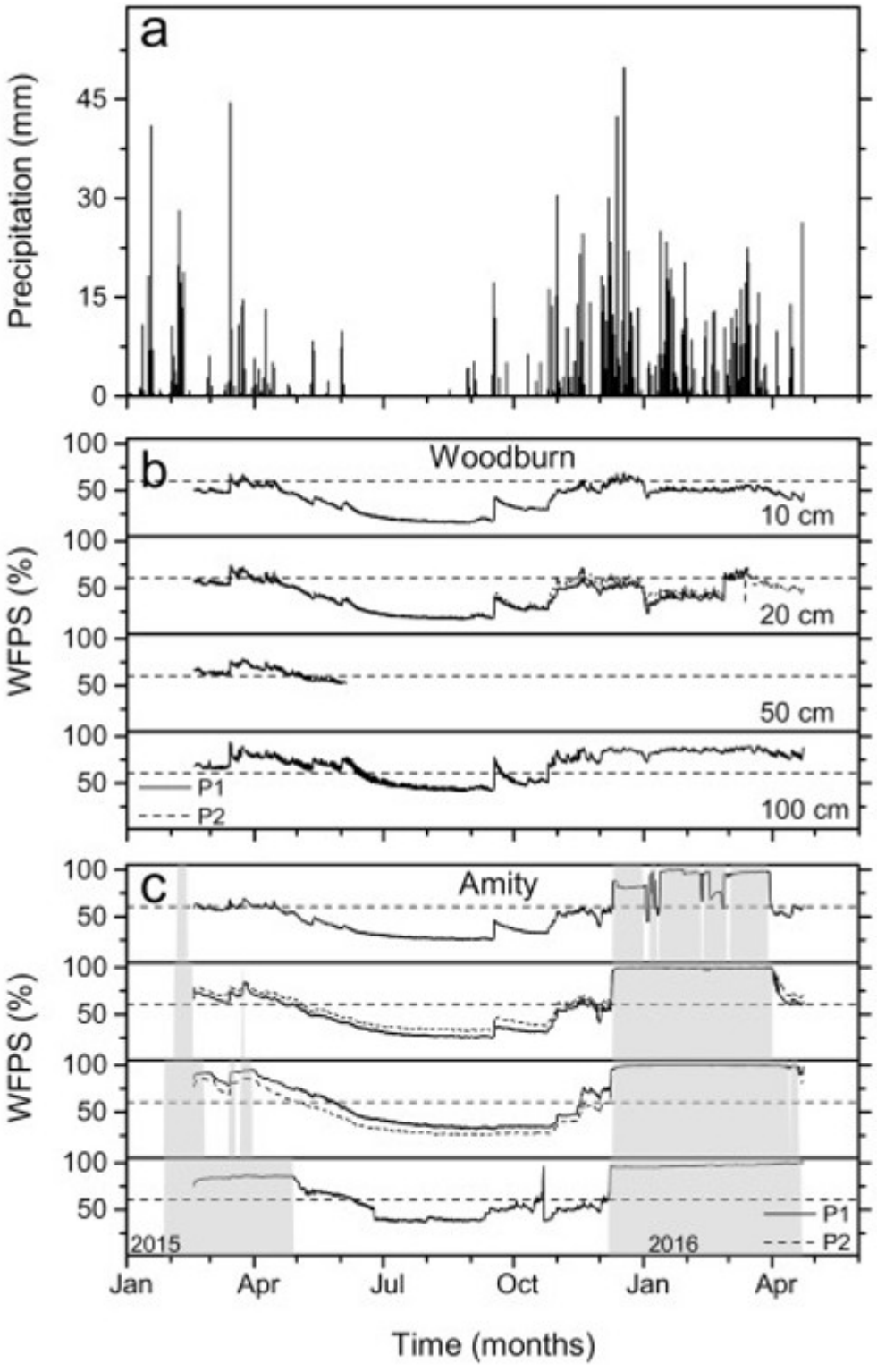

Fig. 2. Time series of precipitation (panel a); and water filled pore space (WFPS) at the Woodburn (Panel b) and Amity (Panel c) soils for the observation period. Shaded area indicates periods where electrodeswere submerged. Depths labeled in the Woodburn panel are the same for the Amity

panel. Percent water filled pore space was calculated using volumetric water content data (measured using Decagon 5TE electrodes and recorded every six hours) and bulk density for each depth. Replicate volumetric water content measurements and subsequent WFPS calculations were made at the Woodburn 10 and 20 cm depths and Amity 20 and 50 cm depths: WFPS calculated from probe 1 = solid and probe 2 = dashed. The horizontal dashed line in each WFPS panel indicates 60% water filled pore space.

3.1.2. Water filled pore space

The fluctuation of water filled pore space (WFPS, given as % of total pore space) over time is presented in Fig. 2 panels b (Woodburn) and c (Amity) together with precipitation (Fig. 2panel a). Panels b and c have a horizontal dashed line to indicate 60% water filled pore space, a value considered as optimal for aerobic microbial activity, with higher WFPS values indicative of restricted oxygen supply (Linn and Doran, 1984). During the dry season, WFPS dropped well below the 60% mark in all soils and at all depths. During wet seasons WFPS exceeded this 60% optimum threshold very briefly at the 10 and 20 cm depths of the Woodburn and extended periods of time in the Amity, reaching full saturation in the Amity during the second wet season. At the 50 and 100 cm depths, the 60% WFPS mark was exceeded throughout the wet seasons, with the distinction that saturation was reached in the Amity but not in the Woodburn.

3.1.3. Soil temperature

Soil temperature for the Woodburn and Amity soils is given in Fig. A.3 b and c as a function of time on the same timescale as precipitation (Fig. A.3 a). In both the Woodburn and Amity, soil temperature increased from February to maximum values in mid-July with a subsequent decline towards seasonal minima in early December, coincident with peaks in precipitation. Changes in temperature from day to day were similar between the two soils, but during periods when the Amity soil was inundated with water, the soil temperature oscillated much less compared to the non-saturated Woodburn, likely owing to the high heat capacity of H_2O. During the relatively dry 2015 winter season, topsoil (10–50 cm) temperatures in the Amity were about 2 degrees C lower than in the Woodburn. Both soils were at the same 10.4 °C at 100 cm. During the much wetter 2016 winter season, both soils had nearly identical and slightly warmer temperatures than in 2015 at all depths.

3.2. Variation of electromotive potentials within one 5-electrode array

Fig. 3 documents the response of individual Pt-electrode potentials to variations in water filled pore space (WFPS). This is illustrated using data from the Pt-electrode array installed at the 20 cm depth in the poorly drained Amity soil. During the 2015 dry season (Fig. 3), with WFPS well below the 60% optimum value for aerobic microbial activity (dashed line in panel 2), the five probes of the array all show near identical potentials close to the theoretical value for the O_2/H_2O couple (805 mV for prevailing conditions, Fig. 1). With the onset of sporadic rainfall events and the concomitant rise of water filled pore space towards the 60% optimum level, potentials begin to drop slightly below 800 mV, but remain close together until the end of

November. As the soil pore volume fills with water in early December of 2015, water filled pore space rapidly rises towards full saturation and potentials start to move towards the 0 to −50 mV region (Fig. 3 panels a, b). Reflecting the conditions in the microenvironments probed by individual electrode tips, individual probes follow separate trajectories, indicating that biogeochemical conditions at the probe tip became increasingly diverse among the 5 electrodes during this period. The biggest spread is reached after the soil begins to dry out again in early April, when two probes (P2 and P4, 20 cm apart) are still at negative potentials (−152 and – 18 mV) while the three others (P1, P3, P5) are consistent with full aeration(+786, +695 and +706 mV). As WFPS returns to the 60% optimum value by the end of April 2016 (Fig. 3 panel b), the potentials at all 5 electrodes of the array reconverge towards a range between +700 and + 800 mV.

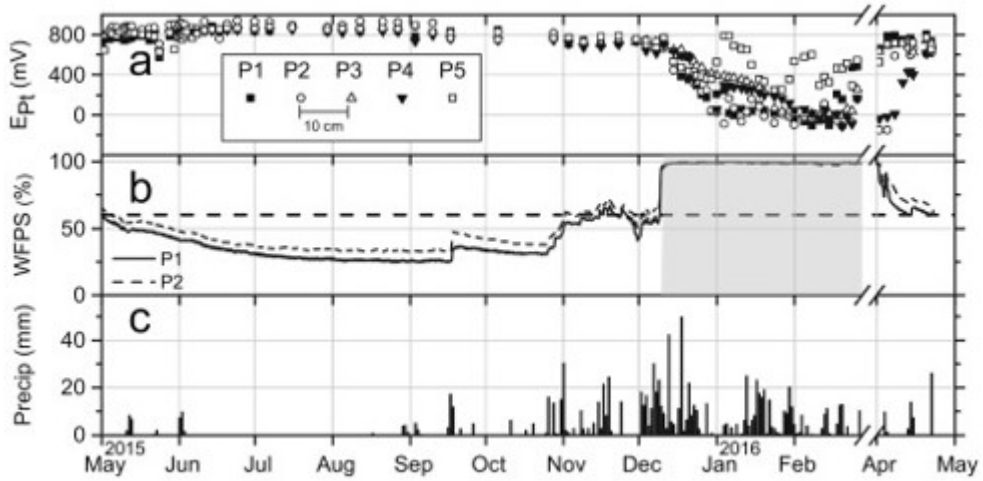

Fig. 3. Time series of platinum probe potentials within the linear array of $n = 5$ probes installed at a depth of 20cm in the Amity soil. Panel a gives E_{Pt} data for each electrode. Inset shows position of electrodes within the array. Panel b gives water filled pore space as a fraction of total pore space (% WFPS). Continuous and dotted line are replicate Decagon 5TE moisture sensors (D1 and D2) as primary moisture data sources. The horizontal dashed line indicates optimum WFPS for microbial activity according to Linn and Doran (1984; 60% WFPS). Shaded area indicates time period where electrodes were submerged. Panel c presents daily precipitation.

3.3. General patterns of electromotive potentials

Plotting time series of electromotive potentials (mean potential per array and observation point; J = 164 observations for Woodburn and Amity; J = 37 observations for Willamette; Fig. 4) reveals unique patterns for each of the three soils. At all depths of the well-drained **Willamette** soil (Fig. 4, panel a), mean potentials remained close to the value for the O_2/H_2O couple throughout the wet season of 2016. Neither temperature nor precipitation events were able to generate significant oscillations of the mean. In the moderately well drained **Woodburn** soil, negative spikes in electromotive potentials occurred during April 2015 and in January 2016 (Fig. 4, panel b) in the topsoil (10 and 20 cm depth), both following periods of high rainfall. Mean potentials stayed above +400 mV at all depths, although individual

probes in the topsoil registered values as low as 137 mV (10 cm) and 224 mV (20 cm).

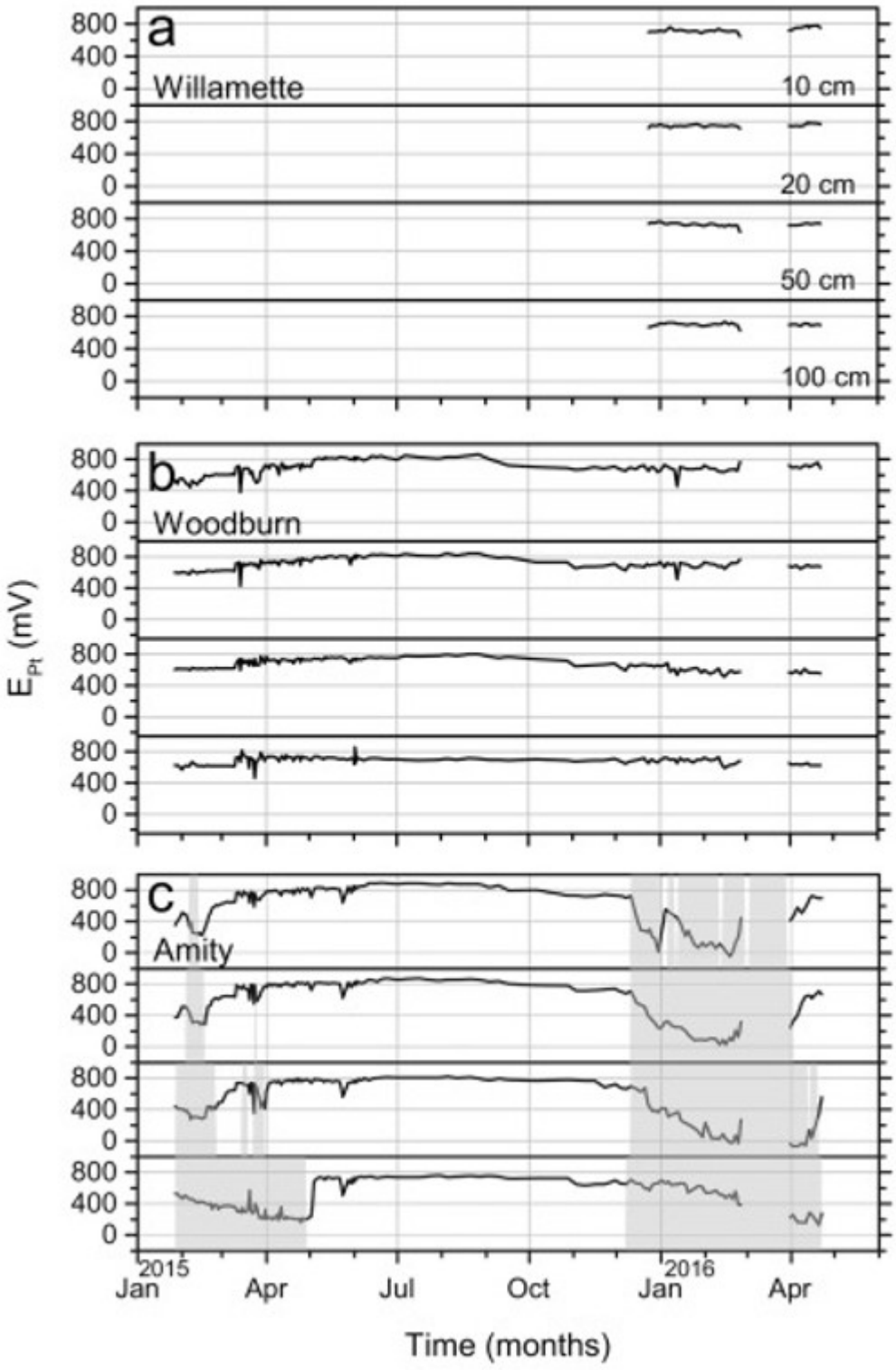

Fig. 4. Time series of platinum electrode potentials (E_{Pt}) across the drainage gradient and for 4 depths (10 cm, 20 cm, 50 cm and 100 cm, labels are not repeated in panels b and c for clarity). Values are

means per array ($n = 5$ electrodes) and observation time point (Table 1). Panel a: well-drained Willamette soil series, Panel b: moderately well drained Woodburn soil, Panel c: poorly drained Amity soil. Shaded area indicates time period where electrodes were submerged.

The largest dynamic of mean electromotive potentials was observed in the poorly drained **Amity** soil, which filled up with water for <2 weeks in the 2014/15 wet season but was constantly inundated for a period of almost 4 months in the 2015/16 wet season (Fig. 4, panel c, periods of water saturation are indicated by gray shading). In the 2015/16 wet season, mean electromotive potential decreased with depth and the lowest mean value was recorded at the 50 cm depth. To our surprise, the lowest electromotive potentials recorded by individual electrodes were not observed in the deepest depth (100 cm: −47 mV), but at a soil depth of 20 cm (−152 mV), followed by the 10 cm depth (−141 mV) and the 50 cm depth (−129 mV). Similar observations were made by Hall et al. (2016), who report more intense microbial Fe reduction in tropical surface soil microsites compared to lesser Fe reduction at greater depths. The time series for the 10, 20 and 50 cm depths resemble each other in their general shape, while the potentials at 100 cm exhibit a distinctly different dynamic, indicating decoupling from any controls acting on the horizons above.

3.4. Trends in functional heterogeneity

Biogeochemical or ‘functional’ heterogeneity was parameterized as the standard deviation of the mean potential within each five-electrode array at each observation time point and plotted for all soils and depths in Fig. 4. In the well-drained **Willamette** soil (receiving the same amount of precipitation as the other two soils), functional heterogeneity was close to zero across all depths and throughout the 2015/2016 wet season (Fig. 5, panel a), despite the fact that rainfall (956 $l\,m^{-2}$, Table A.3) during this period amounted to about 1.9 times the volume of estimated total porosity (500 $l\,m^{-2}\,m^{-1}$ of soil depth, Table A.2). In the **Woodburn**soil, heterogeneity within individual 5-probe arrays was near zero during the dry season, but reached peak values approaching ±231 mV at the end of March 2015 in the topsoil (10 cm depth) and in mid-February 2016 at a depth of 50 cm (±265 mV). Short term changes in soil heterogeneity in the Woodburn topsoil tended to be larger when rain events were more episodic as in the drier wet season of 2014/2015 compared to dampened amplitudes during the much wetter winter of 2015/2016. Heterogeneity in the Woodburn soil declined with depth during the "drier" 2014/2015 wet season, while it increased with depth down to 50 cm during the "wetter" 2015/2016 wet season (Fig. 5, panel b).

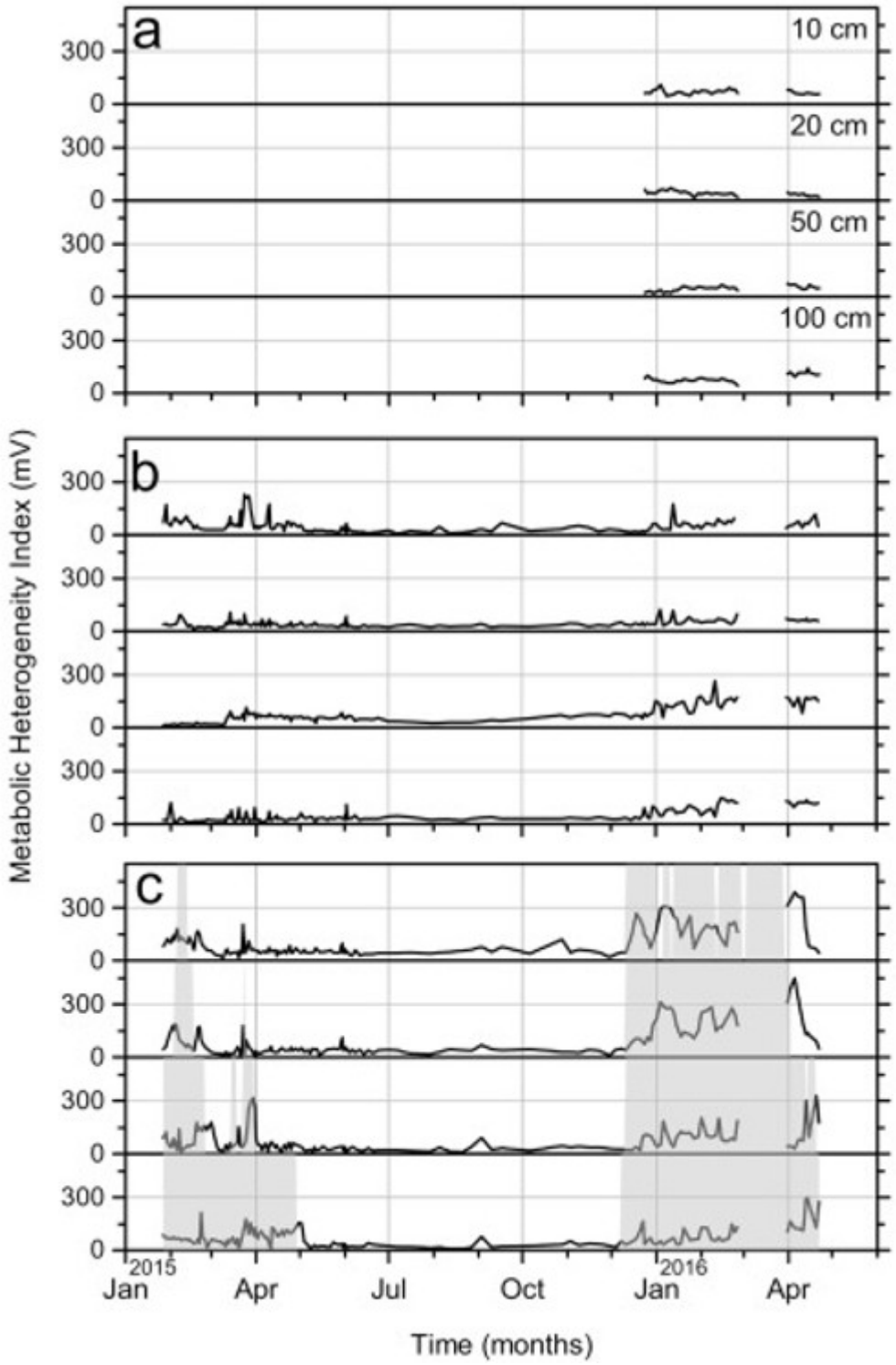

Fig. 5. Time series of metabolic heterogeneity index across the drainage gradient and for 4 depths (10 cm, 20 cm, 50 cm and 100 cm, labels are not repeated in panels b and c for clarity). Values are standard deviations per array ($n = 5$ electrodes) and observation time point (Table 1). Panel a: well-drained Willamette soil series, Panel b: moderately well drained Woodburn soil, Panel c: poorly drained Amity soil. Shaded area indicates full water saturation with electrodes submerged.

The largest measured functional heterogeneity was observed at the 20 cm depth of the poorly drained **Amity** soil, reaching a SD of ±450 mV ($n = 5$) in early April 2016 with a low extreme of −152 mV and a high extreme of +786 mV measured simultaneously by two electrodes only 10 cm apart. Heterogeneity in the Amity exhibited different patterns compared to the Woodburn between the 'dry' 2014/2015 winter and the wetter 2015/2016 winter season. During the 2015 wet season, heterogeneity oscillated around a value of ±70 mV with occasional peaks and an isolated maximum near 300 mV at the 50 cm depth in late March 2015. There was no obvious trend with depth during that period. This was much different during the 2016 wet season, when the Amity topsoil (10 and 20 cm) exhibited large functional heterogeneity over a period of more than five months (Fig. 5, panel c). Both extreme values and amplitudes of heterogeneity declined with depth during that time.

A direct comparison of functional heterogeneity across the three soils is possible by plotting the Metabolic Heterogeneity Index (MHI) as a function of drainage gradient (Fig. 6). This representation emphasizes the correlation between drainage regime and the extent to which soils are structured into biogeochemically distinct microsites. The transient nature of microsites is revealed by comparing metabolic heterogeneity between two wet seasons of different intensity. In the 2015 wet season, MHI decreased with depth in the Woodburn soil (Fig. 7, WO '15) and remained constant with depth in the Amity soil (Fig. 7, AM '15). A completely different picture emerged for the much wetter 2016 winter: heterogeneity increased to a maximum at 50 cm depth in the Woodburn (Fig. 7, WO '16) but had its maximum at the 10 and 20 cm depths in the Amity (Fig. 7, AM '16).

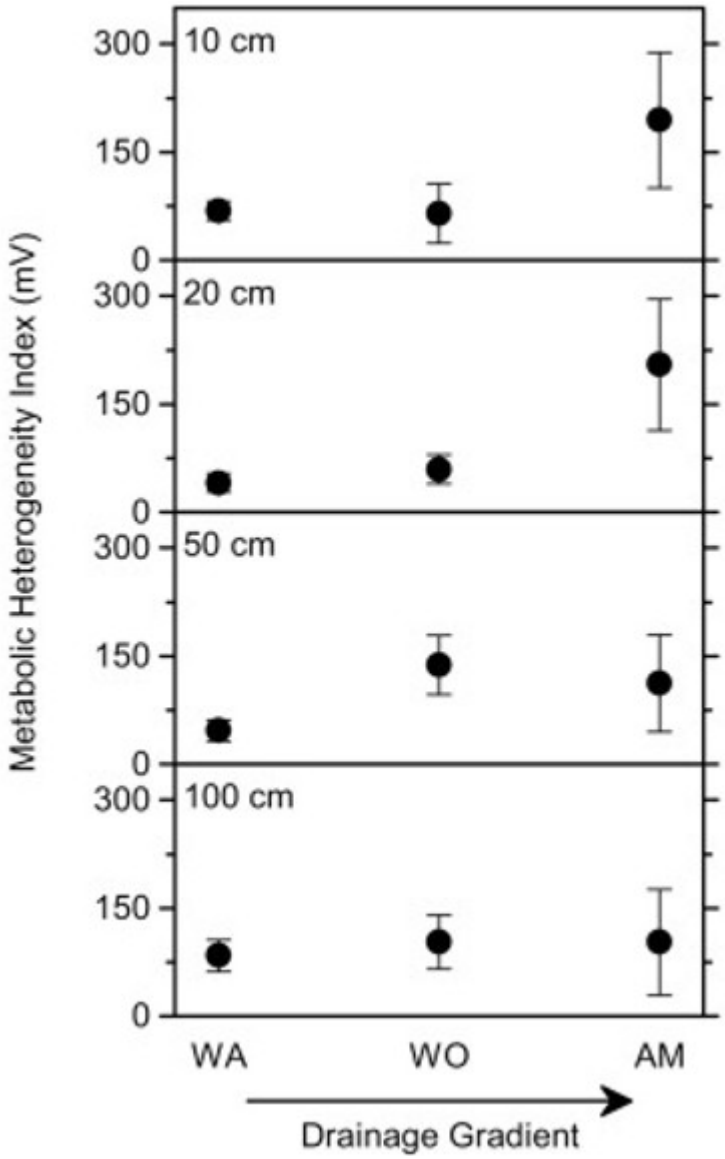

Fig. 6. Variation of metabolic heterogeneity index across the drainage gradient. Values are standard deviations per array ($n = 5$ electrodes) and observation time point. Dots represent mean variability at a given depth for the same subset of matching observation time points from the 2016 wet season (J = 37 observations) across all three soils. Error bars represent the standard deviation of the mean (Table 1). Data are arranged going from well drained (WA) to poorly drained (AM): WA = Willamette, WO = Woodburn, and AM = Amity.

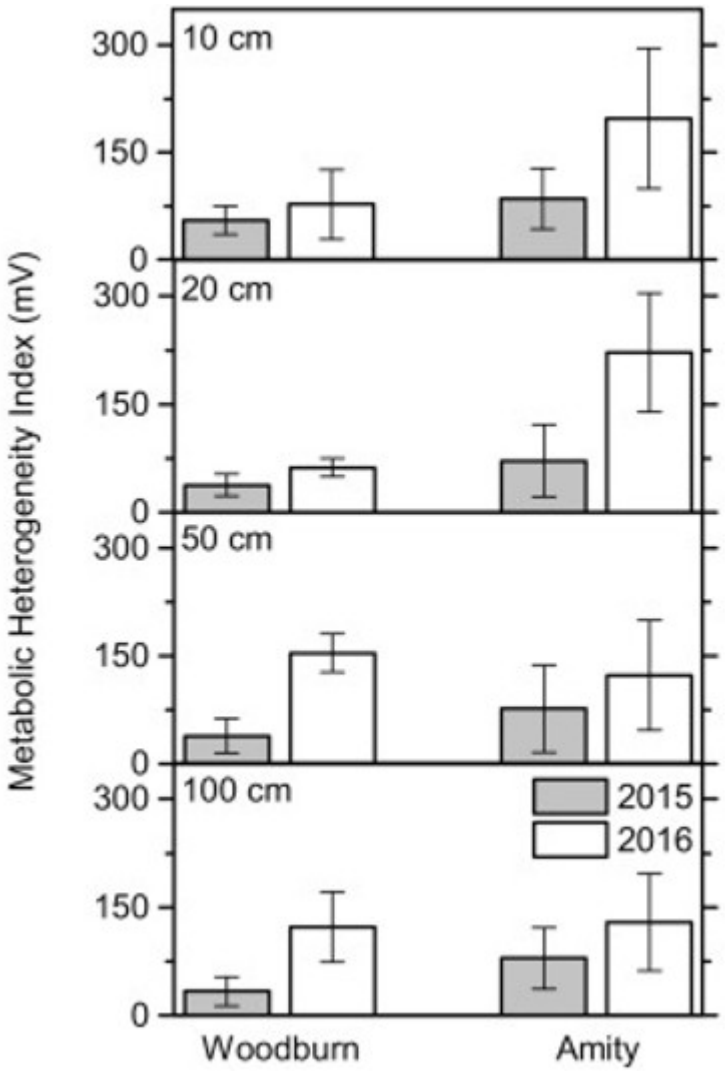

Fig. 7. Variation of metabolic heterogeneity index as a function of intensity of the wet season. Bars represent the mean of the variability at a given depth for the same subset of matching observation time points (J = 18 observations, Table 1) across the 2015 (gray bars) and 2016 (white bars) wet seasons. The error bars are one standard deviation of the mean variability at the given depth for the observation period J (Table 1).

4. Discussion

4.1. Extent and origin of functional heterogeneity in soils

Prompted by the seminal work of Sexstone et al. (1985), and seconded by the growing availability of two- and three-dimensional imaging techniques (Tippkötter et al., 2009; Vereecken et al., 2016), the scientific community has increasingly become mindful of the fact that biogeochemical conditions in soil vary on very small spatial scales. Being able to parameterize the extent of such variation has implications for matter transformations including the biodegradation of carbon substrates (Keiluweit et al., 2016; Keiluweit et al., 2017; Vogel et al., 2015) as it may hold the key to explaining the experimental variability and observed non-linearities associated with these processes (Falconer et al., 2015; Ruamps et al., 2013). Consequently,

quantitative information on functional soil heterogeneity, i.e. on the extent to which ongoing metabolic processes differ among microsites within the same soil horizon, is needed to achieve full mechanistic representation of biogeochemical cycling in soil. The observations we were able to make in the course of this research are in line with previous reports of increasing variability in electromotive potentials across transitions from dry to wet meadow soils, soils in alluvial planes, and soils on pond margins (Dwire et al., 2006; Fiedler and Sommer, 2004; Mansfeldt, 2003). Our observations also concur with previous communications reporting variations in electromotive potentials as a function of soil depth (Dorau and Mansfeldt, 2016; Fiedler and Sommer, 2004). Yang et al. (2006) recorded increasing heterogeneity in electromotive potentials as depth increased in a well-drained silt loam. Thomas et al. (2009) measured electromotive potentials in six different plots on Everglade wetland soils. In all locations monitored, variability in electromotive potentials decreased with depth and they determined that most of the variability could be attributed to fluctuating water tables. Seybold et al. (2002) and Thomas et al. (2009) recorded rapid changes in redox potentials in response to changes in water-table levels in tidal marshes and Everglade wetland soils. However, previous studies did not deploy standardized electrode arrays and hence do not permit a direct parameterization of soil heterogeneity. Our work shows that, through the utilization of geometrically fixed arrays, heterogeneity can be parameterized for the soil volumes defined by the geometry of the array. Deployment of fixed electrode arrays allows the researcher to make comparisons between soil types, soil horizons and assess soil response over time. Doing so allowed us to make the following inference.

a) The degree to which a soil system is divided into biogeochemically distinct microenvironments is not constant over time. The same soil horizon will exhibit vastly different patterns of biogeochemically distinct microsites in two consecutive seasons as a function of changing meteorological conditions.

b) Functional heterogeneity increases with the decreasing hydraulic conductivityassociated with the structural impediments to drainage as reflected in the taxonomic soil drainage class, allowing us to accept the hypothesis that functional soil heterogeneity follows the taxonomic drainage class.

c) There is a strong causal link between soil moisture status and the occurrence, abundance and spatial distribution of biogeochemically distinct microenvironments. Our data show that as a soil system transitions between soil moisture states, the occurrence and diversity of biogeochemical hot spots and hot moments is maximized.

d) In addition to depending on micro-pore structure and moisture, functional heterogeneity shows a threshold around 60% water filled pore space, likely associated with the maximum of aerobic microbial activity often observed in

that moisture range (Linn and Doran, 1984). Below that threshold moisture value, heterogeneity is insensitive to differences in soil texture or precipitation events.

e) Pedological theory dictates that porosity will change with depth, but can be assumed to be constant over the 18-month time frame of our study. This means soil porosityplays an important, yet secondary role for the development of functional heterogeneity in soil.

f) In the case of our soils and dissimilar to the observations of Seybold et al. (2002), variations in temperature did not seem to be as consequential for fluctuations in functional heterogeneity as were changes in water filled pore space.

4.2. A role for Pt-electrode arrays in monitoring metabolic heterogeneity

Conventional Pt-electrode tips probe the electron activity resulting from chemical reactions and associated microbial activity within a sphere of a volume of just a few mm^3 (Fiedler et al., 2007). Compared to lysimeters, trace gas measurement systems, or x-ray tomographic equipment, such Pt-based sensors are cheap, easy to assemble and able to survive deployment in challenging environments for extended times to provide real time information about the status of the soil system and any change thereof.

It is important to realize that the parameter chosen as an index of heterogeneity, the standard deviation of the mean of the probes deployed or Metabolic Heterogeneity Index, will depend on the geometric outline of the electrode array. In the case presented here, we arbitrarily chose a linear, horizontal arrangement of five electrodes spanning a distance of 40 cm, with 10 cm between each electrode tip. This geometric design was kept constant across all soils and depths. Installation will disturb the probed environment, however, interference can be contained by miniaturization of the sensors such as demonstrated in the course of this work (Fig. A.4). Through the utilization of geometrically fixed arrays, heterogeneity can be parameterized for the soil volumes defined by the geometry of the array.

5. Conclusions

With the work presented here, we establish the "Pt-electrode array approach" as a practical means to pursue and further develop the science of biogeochemical soil heterogeneity. To this end, we demonstrate how fixed arrays of sensors capable of probing the electron activity in very small individual volumes can return quantitative information on the extent to which the soil is subdivided in functionally different microsites. The parameter "Metabolic Heterogeneity Index = the standard deviation of the mean electromotive potential within a fixed array of 5 electrodes" allowed us to obtain several insights. Within a horizontal distance of 40 cm and among five microenvironments probed, the functional state of an 'upland' soil may simultaneously include conditions of unrestricted aerobiosis as well as

conditions allowing for sulfate reduction and even methane production (von Fischer et al., 2009). Functional soil heterogeneity is not constant over time, i.e., it cannot be predicted based on soil pore metrics alone (which we assume to remain constant over the observation period). Maximum biogeochemical diversity is most likely encountered in organic matter rich topsoils (Hall et al., 2016) subject to large fluctuations in soil moisture. Rapid draining followed by the gradual drying out of the soil will generate greater functional heterogeneity than rapid rewetting, and functional heterogeneity will be more sensitive to moisture fluctuations than to temperature variations overall. This latter finding could mean that moisture changes associated with climate change could be much more consequential for the broader scale intensity of biogeochemical soil processes than temperature changes. Given the importance of soil heterogeneity for matter transformations in soil systems and the relative ease of technical implementation, we recommend that the standard deviation of mean electromotive Pt-electrode potentials within fixed electrode arrays be further developed as a routine parameter for the characterization of soils in long-term monitoring programs such as Critical Zone Observatories, LTER and NEON sites. This may require standardization of electrode number and the geometry of arrays utilized.

Acknowledgments

This work was supported by the US Department of Energy, Office of Biological and Environmental Research, Terrestrial Ecosystem Program (Award Number DE-FG02-13ER65542). We appreciate the constructive comments of two anonymous reviewers.

References

Austin and Huddleston, 1999

W.E. Austin, J.H. Huddleston**Viability of permanently installed platinum redox electrodes**

Soil Sci. Soc. Am. J., 63 (6) (1999), pp. 1757-1762

Baas Becking et al., 1960

L.G. Baas Becking, I.R. Kaplan, D. Moore**Limits of the natural environment in terms of pH and oxidation-reduction potentials**

J. Geol., 68 (3) (1960), pp. 243-288

Balster and Parsons, 1968

C.A. Balster, R.B. Parsons**Geomorphology and Soils: Willamette Valley**

Oregon State University, Oregon (1968)

Bartlett and James, 1995

R.J. Bartlett, B.R. James**System for categorizing soil redox status by chemical field testing**

Geoderma, 68 (3) (1995), pp. 211-218

Boersma et al., 1972

L. Boersma, D.G. Watts, G.H. Simonson**Soil morphology and water table relations. 1. Annual water table fluctuations**

Soil Sci. Soc. Am. Proc., 36 (1972), pp. 644-648

Bohn, 1971

H.L. Bohn**Redox potentials**

Soil Sci., 112 (1) (1971), pp. 39-45

Brümmer, 1974

G. Brümmer**Redoxpotentiale und Redoxprozesse von Mangan [Eisen und Schwefelverbindungen in hydromorphen Böden und Sedimenten]**

Geoderma, 12 (3) (1974), pp. 207-222

Chacon et al., 2006

N. Chacon, W.L. Silver, E.A. Dubinsky, D.F. Cusack**Iron reduction and soil phosphorus solubilization in humid tropical forests soils: the roles of labile carbon pools and an electron shuttle compound**

Biogeochemistry, 78 (1) (2006), pp. 67-84

Chadwick and Chorover, 2001

O.A. Chadwick, J. Chorover**The chemistry of pedogenic thresholds**

Geoderma, 100 (3–4) (2001), pp. 321-353

Chapelle et al., 1996

F.H. Chapelle, S.K. Haack, P. Adriaens, M.A. Henry, P.M. Bradley**Comparison of E_h and H_2 measurements for delineating redox processes in a contaminated aquifer**

Environ. Sci. Technol., 30 (12) (1996), pp. 3565-3569

Cogger et al., 1992

C.G. Cogger, P.E. Kennedy, D. Carlson**Seasonally saturated soils in the puget lowland II. Measuring and interpreting redox potentials**

Soil Sci., 154 (1) (1992), pp. 50-58

Dorau and Mansfeldt, 2016

K. Dorau, T. Mansfeldt**Comparison of redox potential dynamics in a diked marsh soil: 1990 to 1993 versus 2011 to 2014**

J. Plant Nutr. Soil Sci., 179 (5) (2016), pp. 641-651

Dwire et al., 2006

K.A. Dwire, J.B. Kauffman, J.E. Baham**Plant species distribution in relation to water-table depth and soil redox potential in Montane riparian meadows**

Wetlands, 26 (1) (2006), pp. 131-146

Falconer et al., 2015

R.E. Falconer, G. Battaia, S. Schmidt, P. Baveye, C. Chenu, W. Otten**Microscale heterogeneity explains experimental variability and non-linearity in soil organic matter mineralisation**

PLoS One, 10 (5) (2015), Article e0123774

Faulkner and Patrick, 1992

S.P. Faulkner, W.H. Patrick**Redox processes and daignostic wetland soil indicators in bottomland hardwood forests**

Soil Sci. Soc. Am. J., 56 (1992), pp. 856-865

Faulkner et al., 1989

S.P. Faulkner, W.H. Patrick, R.P. Gambrell**Field techniques for measuring wetland soil parameters**

Soil Sci. Soc. Am. J., 55 (1989), pp. 883-890

Fiedler, 1999

S. Fiedler**In-situ longterm measurements of redox potential in hydromorphic soils, in redox fundamentals**

J. Schüring, H.D. Schulz, W.R. Fischer, J. Böttcher, W.H.M. Duijnisveld (Eds.), Redox Fundamentals, Processes and Measuring Techniques, Springer-Verla, New York (1999), pp. 81-94

Fiedler and Kalbitz, 2003

S. Fiedler, K. Kalbitz**Concentrations and properties of dissolved organic matter in forest soils as affected by the redox regime**

Soil Sci., 168 (11) (2003), pp. 793-801

Fiedler and Sommer, 2000

S. Fiedler, M. Sommer**Methane emissions, groundwater levels and redox potentials of common wetland soils in a temperate-humid climate**

Glob. Biogeochem. Cycles, 14 (4) (2000), pp. 1081-1093

Fiedler and Sommer, 2004

S. Fiedler, M. Sommer**Water and redox conditions in wetland soils - their influence on pedogenic oxides and morphology**

Soil Sci. Soc. Am. J., 68 (1) (2004), pp. 326-335

Fiedler et al., 2007

S. Fiedler, M.J. Vepraskas, J.L. Richardson**Soil redox potential: importance, field measurements, and observations**

94 (2007), pp. 1-54

Gomez et al., 1999

E. Gomez, C. Durillon, G. Rofes, B. Picot**Phosphate adsorption and release from sediments of brackish lagoons: pH, O_2 and loading influence**

Water Res., 33 (10) (1999), pp. 2437-2447

Gotoh and Yamashita, 1966

S. Gotoh, K. Yamashita**Oxidation-reduction potential of a paddy soil *in situ* with special reference to the production of ferrous iron, manganous manganese and sulfide**

Soil Sci. Plant Nutr., 12 (6) (1966), pp. 24-32

Groffman et al., 2009

P.M. Groffman, K. Butterbach-Bahl, R.W. Fulweiler, A.J. Gold, J.L. Morse, E.K. S tander, C.Tague, C. Tonitto, P. Vidon**Challenges to incorporating spatially and temporally explicit phenomena (hotspots and hot moments) in denitrification models**

Biogeochemistry, 93 (1–2) (2009), pp. 49-77

Hall et al., 2016

S.J. Hall, D. Liptzin, H.L. Buss, K. DeAngelis, W.L. Silver**Drivers and patterns of iron redox cycling from surface to bedrock in a deep tropical forest soil: a new conceptual model**

Biogeochemistry, 130 (1–2) (2016), pp. 177-190

Husson, 2012

O. Husson**Redox potential (Eh) and pH as drivers of soil/plant/microorganism systems: a transdisciplinary overview pointing to integrative opportunities for agronomy**

Plant Soil, 362 (1–2) (2012), pp. 389-417

Husson et al., 2016

O. Husson, B. Husson, A. Brunet, D. Babre, K. Alary, J.P. Sarthou, H. Charpenti er, M.Durand, J. Benada, M. Henry**Practical improvements in soil redox potential (Eh) measurement for characterization of soil properties. Application for comparison of conventional and conservation agriculture cropping systems**

Anal. Chim. Acta, 906 (2016), pp. 98-109

James and Brose, 2011

B.R. James, D.A. Brose**Oxidation reduciont phenomena**

Y. Li, Pan Ming Huang, Malcolm E. Sumner (Eds.), Handbook of Soil Sciences: Properties and Processes, CRC Press (2011), pp. 1-24

Jones, 1966

R.H. Jones**Oxidation-reduction potential measurement**

Isa J., 13 (11) (1966), pp. 40-44

Keiluweit et al., 2016

M. Keiluweit, P.S. Nico, M. Kleber, S. Fendorf**Are oxygen limitations under recognized regulators of organic carbon turnover in upland soils?**

Biogeochemistry, 127 (2–3) (2016), pp. 157-171

Keiluweit et al., 2017

M. Keiluweit, T. Wanzek, M. Kleber, P.S. Nico, S. Fendorf**Anaerobic microsites have an unaccounted role in soil carbon stabilization**

Nat. Commun., 8 (1) (2017), p. 1771

Kofod, 1999

M. Kofod**Variance of the redox potential value in two anoxic groundwater systems**

J. Schüring, H.D. Schulz, W.R. Fischer, J. Böttcher, W.H.M. Duijnisveld (Eds.), R edox: Fundamentals, Processes and Applications, Springer-Verlag (1999), pp. 120-134

Kravchenko et al., 2015

A.N. Kravchenko, W.C. Negassa, A.K. Guber, M.L. Rivers**Protection of soil carbon within macro-aggregates depends on intra-aggregate pore characteristics**

Sci. Rep., 5 (2015), p. 16,261

Kuzyakov and Blagodatskaya, 2015

Y. Kuzyakov, E. Blagodatskaya**Microbial hotspots and hot moments in soil: concept & review**

Soil Biol. Biochem., 83 (2015), pp. 184-199

Linn and Doran, 1984

D.M. Linn, J.W. Doran**Effect of water-filled pore-space on carbon-dioxide and nitrous-oxide production in tilled and nontilled soils**

Soil Sci. Soc. Am. J., 48 (6) (1984), pp. 1267-1272

Mansfeldt, 2003

T. Mansfeldt**In situ long-term redox potential measurements in a dyked marsh soil**

J. Plant Nutr. Soil Sci., 166 (2) (2003), pp. 210-219

Mansfeldt, 2004

T. Mansfeldt**Redox potential of bulk soil and soil solution concentration of nitrate, manganese, iron, and sulfate in two Gleysols**

J. Plant Nutr. Soil Sci., 167 (1) (2004), pp. 7-16

Masscheleyn et al., 1990

P.H. Masscheleyn, R.D. Delaune, W.H. Patrick**Transformations of selenium as affected by sediment oxidation reduction potential and pH**

Environ. Sci. Technol., 24 (1) (1990), pp. 91-96

McClain et al., 2003

M.E. McClain, E.W. Boyer, C.L. Dent, S.E. Gergel, N.B. Grimm, P.M. Groffman, S.C. Hart, J.W. Harvey, C.A. Johnston, E. Mayorga, W.H. McDowell, G. Pinay**Bi ogeochemical hot spots and hot moments at the interface of terrestrial and aquatic ecosystems**

Ecosystems, 6 (4) (2003), pp. 301-312

McKeague, 1965

J.A. McKeague**Relationship od water table and Eh to properties of three clay soils in the Ottawa Valley**

Can. J. Soil Sci., 45 (1965), pp. 49-62

Megonigal et al., 1993

J.P. Megonigal, W.H. Patrick, S.P. Faulkner**Wetland identification in seasonally flooded forest soils - soil morphology and redox dynamics**

Soil Sci. Soc. Am. J., 57 (1) (1993), pp. 140-149

Menne et al., 2012

M.J. Menne, I. Durre, R.S. Vose, B.E. Gleason, T.G. Houston**An overview of the global historical climatology network-daily database**

J. Atmos. Ocean. Technol., 29 (7) (2012), pp. 897-910

Negassa et al., 2015

W.C. Negassa, A.K. Guber, A.N. Kravchenko, T.L. Marsh, B. Hildebrandt, M.L. Rivers**Properties of soil pore space regulate pathways of plant residue decomposition and community structure of associated bacteria**

PLoS One, 10 (4) (2015), Article e0123999

Nordstrom and Wilde, 2005

D.K. Nordstrom, F.D. Wilde**Field measurements: U.S. Geological Survey Techniques of Water-Resources Investigations, book 9, chap. A6, sec. 6.5**

(2005)

accessed January 6, 2017, at http://pubs.water.usgs.gov/twri9A6/

Patrick and Mahapatra, 1968

W.H. Patrick, I.C. Mahapatra**Transformation and availability to rice of nitrogen and phosphorus in waterlogged soils**

Adv. Agron., 20 (1968), pp. 323-359

Patrick and Turner, 1968

W.H. Patrick, F.T. Turner**Effect of redox potential on manganese transformation in waterlogged soil**

Nature, 220 (5166) (1968), pp. 476-478

Patrick and Jugsujinda, 1992

W.H. Patrick, A. Jugsujinda**Sequential reduction and oxidation of inorganic nitrogen, manganese, and iron in flooded soil**

Soil Sci. Soc. Am. J., 56 (4) (1992), pp. 1071-1073

Patrick et al., 1996

W.H. Patrick, R.P. Gambrell, S.P. Faulkner**Redox measurements of soils**

D.L. Sparks, A.L. Page, P.A. Helmke, R.H. Loeppert, P.N. Soltanpour, M.A. Tab atabai, C.T. Johnston, M.E. Sumner (Eds.), Methods of Soil Analysis. Part 3. Chemical Methods, Soil Science Society of America Inc., Madison, USA (1996), pp. 1255-1273

Peiffer, 1992

S. Peiffer**Redox measurements in aqueous solutions - a theoretical approach to data interpretation, based on electrode kinetics**

J. Contam. Hydrol., 10 (1) (1992), pp. 1-18

Peiffer, 1999

S. Peiffer**Characterization of the redox state of aqueous systems: towards a problem-oriented approach**

J. Schüring, H.D. Schulz, W.R. Fischer, J. Böttcher, W.H.M. Duijnisveld (Eds.), R edox Fundamentals, Processes and Measuring Techniques, Springer-Verla, New York (1999), pp. 24-39

Rabenhorst, 2009

M.C. Rabenhorst**Making soil oxidation–reduction potential measurements using multimeters**

Soil Sci. Soc. Am. J., 73 (6) (2009), p. 2198

Ruamps et al., 2013

L.S. Ruamps, N. Nunan, V. Pouteau, J. Leloup, X. Raynaud, V. Roy, C. Chenu**R egulation of soil organic C mineralisation at the pore scale**

FEMS Microbiol. Ecol., 86 (1) (2013), pp. 26-35

Schoeneberger et al., 2012

P.J. Schoeneberger, D.A. Wysocki, E.C. Benham, S.S. Staff

N.R.C. Service (Ed.), Field Book for Describing and Sampling Soils, Version 3.0, National Soil Survey Center, Lincoln, NE (2012)

Sexstone et al., 1985

A.J. Sexstone, N.P. Revsbech, T.B. Parkin, J.M. Tiedje**Direct measurement of oxygen profiles and denitrification rates in soil aggregates**

Soil Sci. Soc. Am. J., 49 (3) (1985), pp. 645-651

Seybold et al., 2002

C.A. Seybold, W. Mersie, J.Y. Huang, C. McNamee**Soil redox, pH, temperature, and water-table patterns of a freshwater tidal wetland**

Wetlands, 22 (1) (2002), pp. 149-158

Sigg, 1999

L. Sigg**Redox potential measurements in natural waters: significance: concepts and problems**

J. Schüring, H.D. Schulz, W.R. Fischer, J. Böttcher, W.H.M. Duijnisveld (Eds.), R edox Fundamentals, Processes and Measuring Techniques, Springer-Verlag, New York (1999), pp. 1-11

Sposito, 2016

G. Sposito**The Chemistry of Soils**

(3rd ed.), Oxford University Press, New York (2016)

Staff, 2015

S.S. Staff**Examination and description of soils**

C. Ditzler, L.T. West (Eds.), Soil Survey Manual, U.S. Department of Agriculture, Natrual Resources Conservation Service (2015)

Stumm, 1966

W. Stumm**Redox Potential as an Environmental Parameter - Conceptual Significance and Operational Limitation, Advances in Water Pollution Research**

Proceedings of the 3rd Intl Conference, Munich, Germany (1966), pp. 283-298

Thomas et al., 2009

C.R. Thomas, S. Miao, E. Sindhoj**Environmental factors affecting temporal and spatial patterns of soil redox potential in Florida Everglades wetlands**

Wetlands, 29 (4) (2009), pp. 1133-1145

Tippkötter et al., 2009

R. Tippkötter, T. Eickhorst, H. Taubner, B. Gredner, G. Rademaker**Detection of soil water in macropores of undisturbed soil using microfocus X-ray tube computerized tomography (µCT)**

Soil Tillage Res., 105 (1) (2009), pp. 12-20

Vepraskas and Faulkner, 2001

M.J. Vepraskas, S.P. Faulkner**Morphological features of seasonally reduced soils**

Wetland Soils—Genesis, Hydrology, Landscapes and Classification, Lewis Publishers, Boca Raton, FL(2001)

Vereecken et al., 2016

H. Vereecken, A. Schnepf, J.W. Hopmans, M. Javaux, D. Or, D.O.T. Roose, J.Vanderborght, M.H. Young, W. Amelung, M. Aitkenhead, S.D. Allison, S. Assoulin e, P. Baveye, M. Berli, N. Bruggemann, P. Finke, M. Flury, T. Gaiser, G. Govers , T. Ghezzehei, P. Hallett, H.J.H. Franssen, J.Heppell, R. Horn, J.A. Huisman, D. Jacques, F. Jonard, S. Kollet, F. Lafolie, K. Lamorski, D. Leitner, A.McBratney, B. Minasny, C. Montzka, W. Nowak, Y. Pachepsky, J. Padarian, N. Romano, K. Roth, Y.Rothfuss, E.C. Rowe, A. Schwen, J. Simunek, A. Tiktak, J. Van Dam, S.E.A.T.M. van der
Zee, H.J. Vogel, J.A. Vrugt, T. Wohling, I.M. Young**Modeling soil processes: review, key challenges, and new perspectives**

Vadose Zone J., 15 (5) (2016), pp. 1-57

Vogel et al., 2015

L.E. Vogel, D. Makowski, P. Garnier, L. Vieublé-Gonod, Y. Coquet, X. Raynaud, N. Nunan, C.Chenu, R. Falconer, V. Pot**Modeling the effect of soil meso- and macropores topology on the biodegradation of a soluble carbon substrate**

Adv. Water Resour., 83 (2015), pp. 123-136

von Fischer et al., 2009

J.C. von Fischer, G. Butters, P.C. Duchateau, R.J. Thelwell, R. Siller**In situ measures of methanotroph activity in upland soils: a reaction-diffusion model and field observation of water stress**

J. Geophys. Res., 114 (G1) (2009)

Wang et al., 1993

Z.P. Wang, R.D. DeLaune, W.H. Patrick, P.H. Masscheleyn**Soil redox and pH effects on methane production in a flooded rice soil**

Soil Sci. Soc. Am. J., 57 (2) (1993), pp. 382-385

Yang et al., 2006

J. Yang, Y. Hu, R. Bu**Microscale spatial variability of redox potential in surface soil**

Soil Sci., 171 (10) (2006), pp. 747-753

Young and Crawford, 2004

I.M. Young, J.W. Crawford**Interactions and self-organization in the soil-microbe complex**

Science, 304 (5677) (2004), pp. 1634-1637

Yu et al., 2006

K. Yu, S.P. Faulkner, W.H. Patrick Jr.**Redox potential characterization and soil greenhouse gas concentration across a hydrological gradient in a Gulf coast forest**

Chemosphere, 62 (6) (2006), pp. 905-914

Yu et al., 2007

K. Yu, F. Böhme, J. Rinklebe, H.-U. Neue, R.D. DeLaune**Major biogeochemical processes in soils-a microcosm incubation from reducing to oxidizing conditions**

Soil Sci. Soc. Am. J., 71 (4) (2007), pp. 1406-1417